CHAPTER 2

Methodology

The workflow used in this seismic pre-stack simultaneous inversion study consisted of five main steps; rock physics analysis, well tie and wavelet extraction, low frequency modelling, seismic simultaneous inversion and lithofacies classification. The details for each step are described as follows.

2.1 Rock Physics Analysis

Rock physics analysis is typically used to define the relationships of elastic properties to achieve the understanding of rock properties which is directly related to interpreting seismic signatures. The workflow consisted of well log conditioning, lithology log interpretation, fluid replacement modelling, AVO classification and log upscaling.

Well log data, such as sonic, shear sonic and bulk density logs were the most important datasets used in this part of the study. Crossplots of well log data and calculated elastic properties were used to evaluate the potential of lithology and/or fluid classifications for seismic reservoir characterization. For this purpose, proper QC and well log conditioning were applied. The log data conditioning included bad data removal, log splicing and other quality improvements. This step also involved shear wave velocity prediction in wells without measured shear wave sonic log data. Shear wave sonic log data were estimated using compressional wave velocity (Vp) and shear wave velocity (Vs) relationships derived from available well log data. The empirical relationships published by Castagna et al. (1985), demonstrated a simple systematic relationship between Vp and Vs for brine filled sandstone, using laboratory experiments. Greenberg and Castagna (1992) further developed these relationships by also accounting for other sedimentary rocks, defined by four trends for commonly

ลิขสิทธิ์มหาวิทยาลัยเชียงใหม่
Copyright© by Chiang Mai University
All rights reserved

occurring (brine bearing) minerals. The equations (Simm and Bacon, 2014) and Vp-Vs crossplots of these relationships were displayed in Figure 2-1.

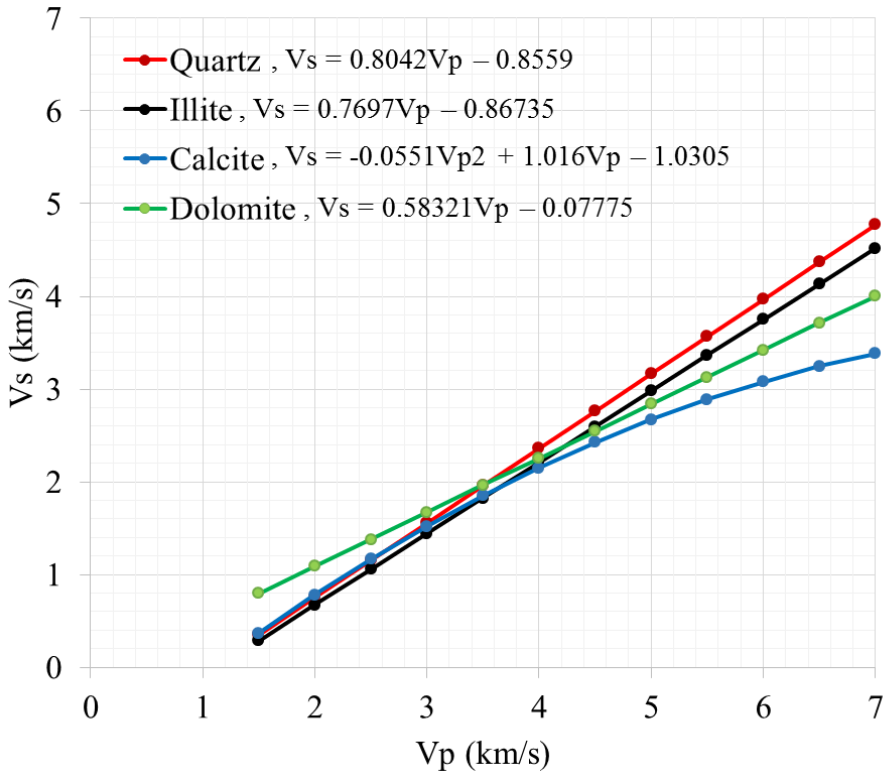

Figure 2-1 Crossplot showing Greenberg and Castagna (1992) Vp –Vs relation of quartz, illite, calcite and dolomite.

The study area contained varying lithofacies, such as sandstone, siltstone, shale, claystone, calcareous claystone, marl, limestone, calcarenite etc. Lithology logs were predicted using gamma ray log cut-off values, and interpreted composite logs. To simplify, the lithologies was classified as sandstone, shale and carbonate facies. Sandstone facies contained sandstones and siltstones. Claystone, calcareous claystone and shale were classified as Shale facies. Carbonate facies consisted of marls, limestones and calcarenite.

A key to interpretation of seismic amplitude variations depends on the understanding of how the rock properties were affected by fluid fill. This was achieved by applying a specific workflow (Figure 2-2), also referred to as fluid replacement modelling (FRM). Results were related to seismic data by evaluating the potential of seismic-driven fluid discrimination and AVO classification with depth.

ลิขสิทธิ์มหาวิทยาลัยเชียงใหม่
Copyright© by Chiang Mai University
All rights reserved

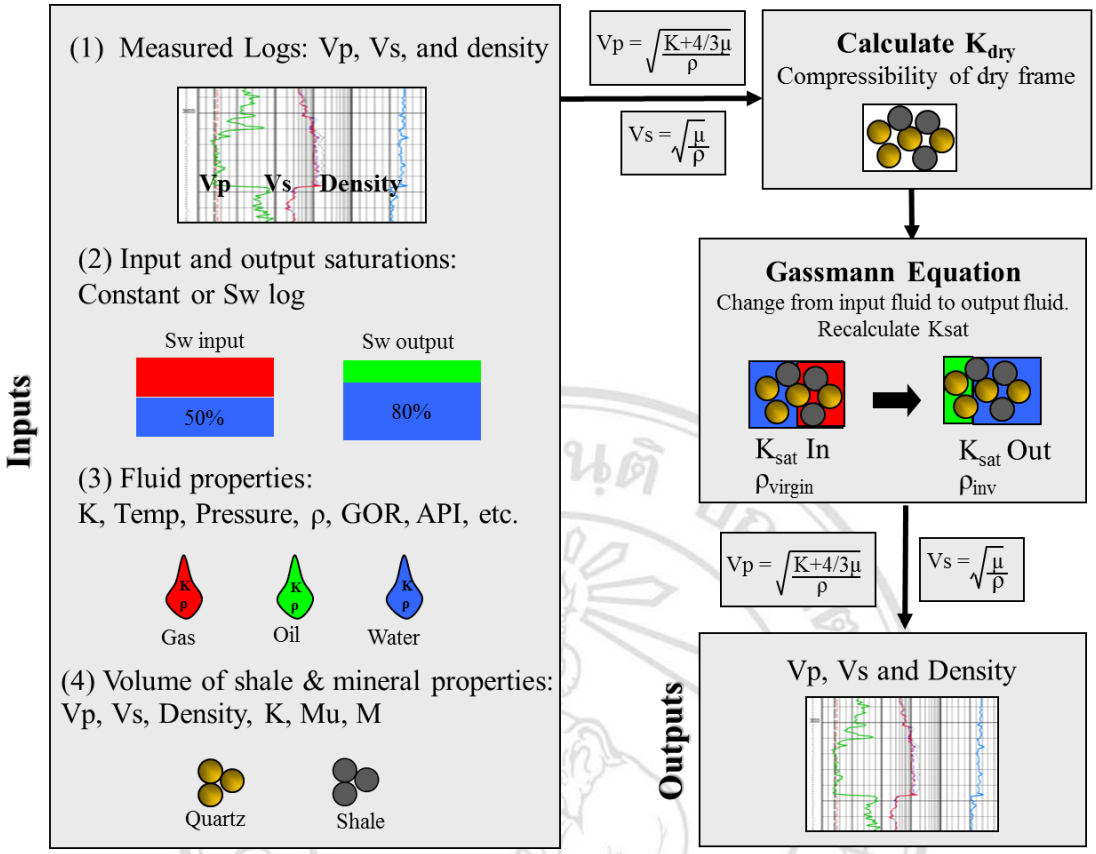

Figure 2-2 Fluid replacement modelling (FRM) workflow using Gassmann's Equation.

The basis of FRM is the well-known Gassmann's equation (Gassmann, 1951), which describes rocks as a two-phase medium, consisting of mineral matrix and fluid. The equations can be written as Equations 2-5 and 2-6:

$$\frac{K_{sat}}{K_0 - K_{sat}} = \frac{K_d}{K_0 - K_d} + \frac{K_{fl}}{\phi(K_0 - K_{fl})} \quad (2\text{-}5),$$

$$\mu_{sat} = \mu_d \quad (2\text{-}6),$$

where K_{sat} is the bulk modulus of the fluid saturated rock, K_0 is the bulk modulus of the matrix material, K_d is the bulk modulus of the dry rock frame, K_{fl} is the bulk modulus of the pore fluid, ϕ is the effective porosity, μ_{sat} is the shear modulus of the fluid saturated rock and μ_d is the shear modulus of the dry rock frame. The assumptions in the Gassmann's equation are that (Simm and Bacon, 2014):

- the solid model is homogeneous and isotropic,

ลิขสิทธิ์มหาวิทยาลัยเชียงใหม่
Copyright© by Chiang Mai University
All rights reserved

- all the pore space is in communication,
- wave-induced pressure changes throughout the pore space have time to equilibrate during a seismic period (the low frequency assumptions),
- the fluid that fills in the pore space is frictionless (i.e. low viscosity),
- no coupling between solid and fluid phases.

Vp, Vs and density logs were used in combination with known rock property logs, such as porosity and water saturation. Fluid substitution was applied for different fluid types in the relevant reservoir sections. The initial Vp, Vs and density logs are all affected by the in-situ saturation and fluid types. The bulk moduli parameter of the dry rock frame is a significant part of the FRM calculation, and was inverted from the other input data. Gassmann's equation was applied to calculate final fluid saturated bulk modulus. The final Vp, Vs and density of replaced fluid were calculated using Equations 2-7 and 2-8:

$$Vp = \sqrt{\frac{K + {}^{4}/_{3}\mu}{\rho}} \quad (2\text{-}7),$$

$$Vs = \sqrt{\frac{\mu}{\rho}} \quad (2\text{-}8),$$

where K is bulk modulus, μ is shear modulus and ρ is density.

Amplitude versus offset (AVO) using blocky models was analyzed well log data for AVO classification. The analysis was considered for three cases to evaluate fluid sensitivity. These cases were shale over gas sand, shale over brine sand and shale over in-situ fluid saturated sand. The AVO classes can be identified based on characters amplitude response on each incident angle as shown in Figure 2-3.

ลิขสิทธิ์มหาวิทยาลัยเชียงใหม่
Copyright© by Chiang Mai University
All rights reserved

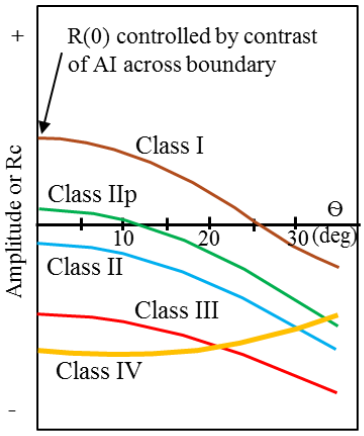

Class	Gradient	Absolute Amplitudes	Notes
I	-	Far < R(0)	+ve R(0), may have phase reversal
IIp	-	Far > R(0)	+ve R(0), phase reversal
II	-	Far > R(0)	Low amplitude at R(0)
III	-	Far > R(0)	Relatively high amplitude at R(0)
IV	+	Far < R(0)	Very high amplitude at R(0)

Figure 2-3 The AVO classes (modified from Simm and Bacon, 2014).

AVO was regularly divided into 4 classes, 3 classes (Class I, II, and III) were introduced by Rutherford and Williams (1989) and 1 class (Class IV) was introduced by Castagna and Swan (1997). The intercept is the acoustic impedance contrast while the sign and magnitude of the AVO gradient is determined principally by the contrast of shear wave velocity across boundary (Castagna et al., 1998; Castagna and Smith, 1994; Simm and Bacon, 2014). AVO gradient is considered the slope change in amplitude with sin2θ. As Simm and Bacon (2014) addressed, positive AVO is applied to either positive or negative amplitudes which are increasing in magnitude with angle. While, negative AVO is defined to amplitude decrease with increasing incident angle. Further crossplot between intercept and AVO gradient were used to categorize the AVO classes (Figure 2-4), as will be discussed.

Class I responses is categorized by positive intercept and negative AVO gradient (the reflection coefficient is positive and decrease with angle). Class II response has a small positive intercept and a negative AVO gradient, while Class IIp is characterized by a small negative intercept and a negative AVO gradient. Phase reversal is a common characteristic of Class IIp, and due to the ambiguity of the small intercept can also occur for class II. Class III response has large negative normal incidence coefficient with negative AVO gradient. Typically, Class II and Class III are difficult to categorize due to what is meant by “small” normal incidence reflection coefficient in the definition of class II (Simm and Bacon, 2014). Large negative normal incidence reflection coefficient and decreasing amplitude with offset is classified as Class IV.

ลิขสิทธิ์มหาวิทยาลัยเชียงใหม่
Copyright© by Chiang Mai University
All rights reserved

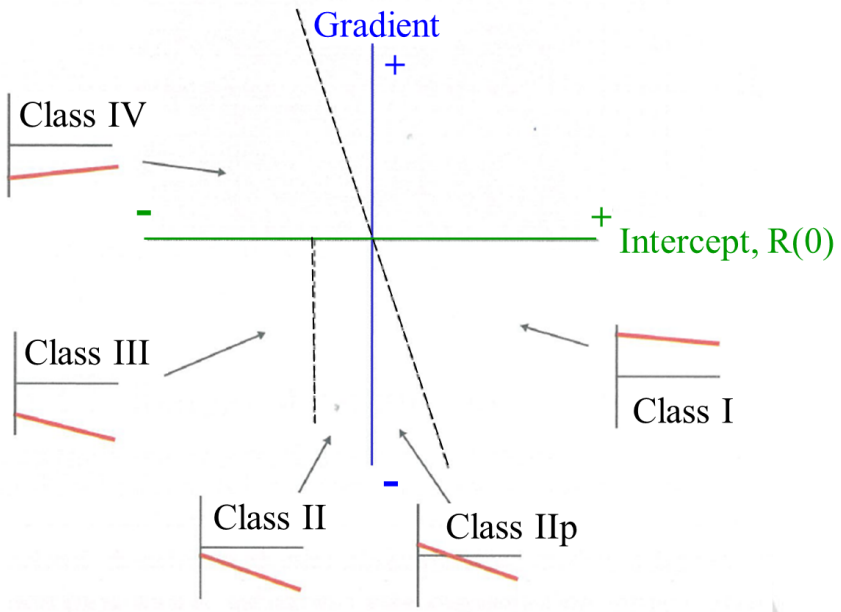

Figure 2-4 AVO classes were categorized using crossplot of intercept and AVO gradient (modified after Simm and Bacon, 2014).

2.2 Well Tie and Wavelet Extraction

The workflow used for well tie and wavelet extraction is summarized by Figure 2-5. The process was started by using the raw check shot data to define an initial time-depth relationship. Computed synthetic seismograms at each well were used to tie seismic data in time to well log data in depth. Initial synthetic seismogram was computed by convolving reflection coefficient log with the initial wavelet, extracted from either the mid angle or full angle seismic stack due to mid angle stack was represented moderately amplitude and reduced the variation of extracted wavelet shape between near and far angle stack. Correlation coefficients were computed to determine the match between seismic and synthetic traces at all well locations within the study area. A correlation factor of 1 represented perfect match, while a correlation factor of 0 represented no correlation. Both time bulk shifts and stretch-squeeze to modify the drift curve were applied to improve the well to seismic tie. This was followed by wavelet extraction for all angle stacks. These wavelets were used to calculate improved synthetic traces to further adjust and optimize the time-depth relations. A final time-depth relationship was optimized, considering from final well to seismic ties for all angle stacks.

ลิขสิทธิ์มหาวิทยาลัยเชียงใหม่
Copyright© by Chiang Mai University
All rights reserved

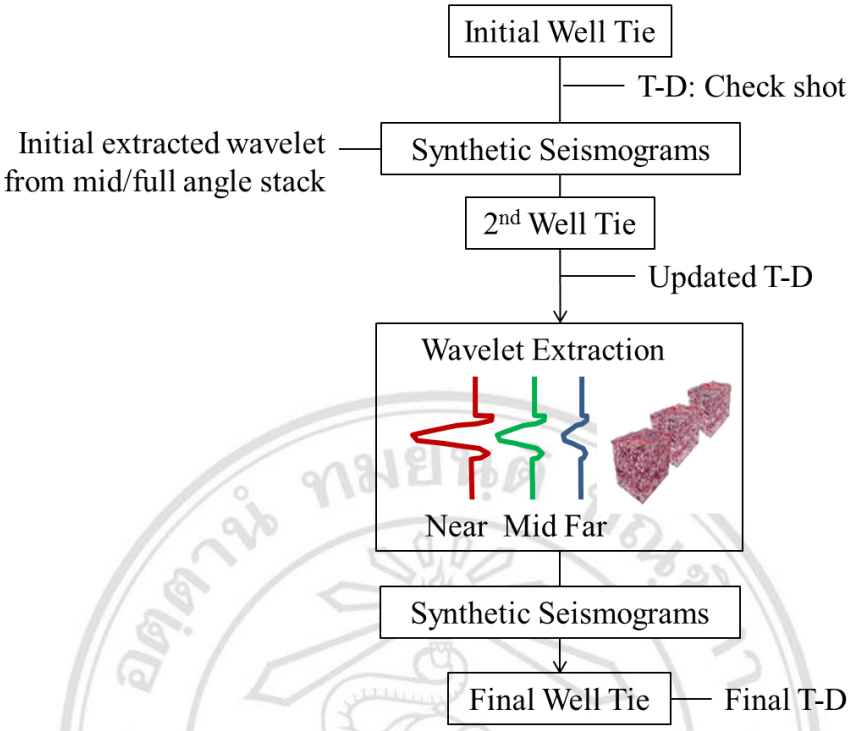

Figure 2-5 Well tie and wavelet extraction workflow.

Final wavelet extraction for all available angle stacks was performed at all well locations. Final multi-well (average) wavelets were generated for each angle stack to be the input for the seismic inversion. Moreover, seismic resolution and detectability were included in this stage to evaluate the quality of the input seismic data. Dominant frequency was derived from the amplitude spectrum of the wavelet extracted from the seismic data. The result was used to estimate seismic resolution (tuning thickness) within the target window by using Equations 2-9 and 2-10:

$$\lambda = \frac{v}{f} \qquad (2\text{-}9),$$

$$\text{Tuning thickness} = \lambda/4 \qquad (2\text{-}10),$$

where v is average velocity calculated from sonic (Vp) log data, f is the derived dominant frequency ,and λ is the wavelength.

ลิขสิทธิ์มหาวิทยาลัยเชียงใหม่
Copyright© by Chiang Mai University
All rights reserved

2.3 Low Frequency Modelling

To transform relative inverted elastic properties to the absolute inverted properties (Figure 2-6), low frequency models were required to incorporate as input in seismic simultaneous inversion process.

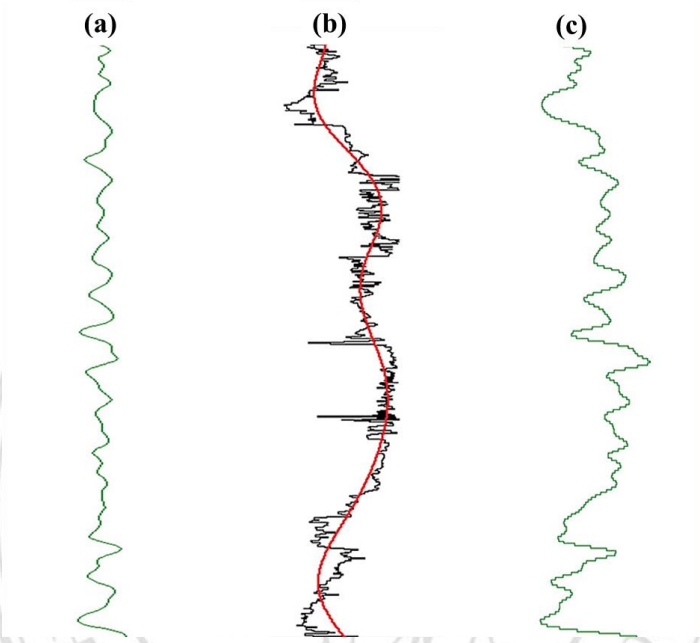

Figure 2-6 (a) Relative impedance trace derived from seismic, (b) Low frequency trend (in red) derived from impedance log (in black), and (c) Absolute impedance trace after addition of the low frequency trend (modified from Chopra and Sharma, 2012).

As seismic data do not contain the low frequencies, which is a limitation caused by instrumentation and seismic acquisition geometries. The missing of low frequency of seismic data; ranged from 0 Hz to the lowest end of the seismic frequency spectrum, is estimated from other sources of available data, such as seismic stacking velocities and well log data, and further constrained by interpreted seismic horizons. This is referred to as a low frequency model (LFM), and is a significant part of the input when carrying out an absolute seismic inversion. The combination of a LFM and the seismic dataset completes the frequency range from 0 Hz to the highest end of the seismic frequency spectrum (Figure 2-7).

ลิขสิทธิ์มหาวิทยาลัยเชียงใหม่
Copyright© by Chiang Mai University
All rights reserved

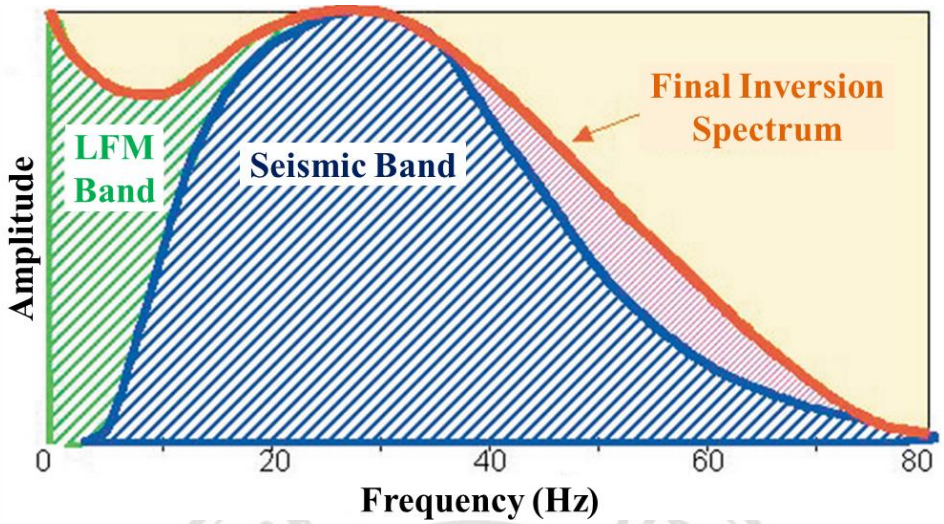

Figure 2-7 Low frequency model was filled the bandwidth of seismic frequency range (modified from Pendrel and Van Riel, 2000).

The low frequency models (LFM) were built in the time domain using a combination of elastic properties i.e. acoustic impedance, shear impedance, and density those were derived by combining well log data and trends extracted from final stacking velocities. Low frequency modelling was divided into two parallel workflows which comprised of an ultra-low frequency model (ULFM) from seismic data and a low frequency model from well data as described in Figure 2-8.

Seismic stacking velocities were firstly converted to interval velocities using Dix formula. Vp versus AI, Vp versus SI and Vp versus density crossplots using all wells data points were fitted by the regressions to obtain the relationships. Then, seismic interval velocity further transformed to elastic properties using the derived relationships which were the initial ultra-low frequency models (acoustic impedance, shear impedance and density). The initial ultra-low frequency models were extracted at wells and patched with well data over zone of interest. Residual logs of elastic properties were computed using patched well acoustic impedance minus extracted initial ultra-low frequency model to calibrate the models and achieve the calibrated ultra-low frequency models.

ลิขสิทธิ์มหาวิทยาลัยเชียงใหม่
Copyright © by Chiang Mai University
All rights reserved

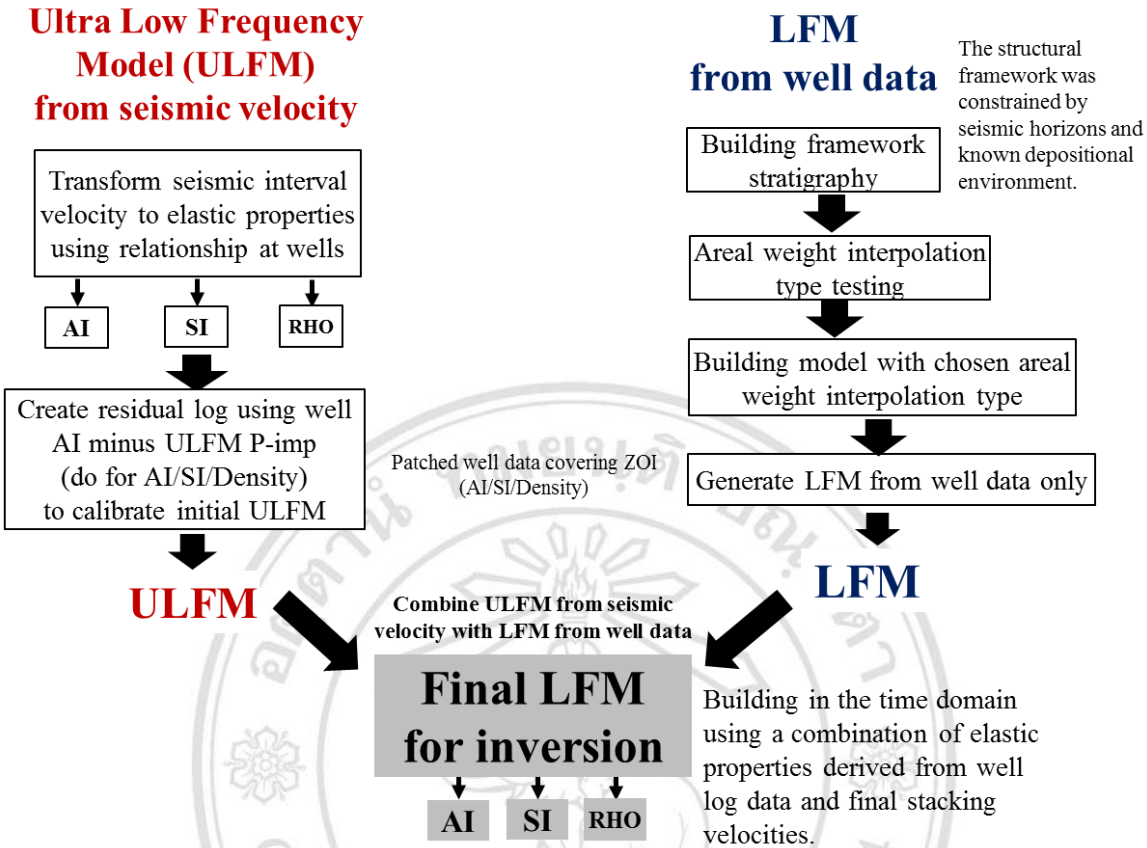

Figure 2-8 Low frequency modelling workflow.

The low frequency modelling from well data were constrained by a stratigraphic framework, built from interpreted seismic horizons. The internal layering between interpreted horizons within this framework was based on the known depositional environments between these horizons. Well log data of acoustic impedance, shear impedance and density were patched with the ultra-low frequency covering the zone of interest and interpolated along the structural framework to extract low frequency models from well data. The final low frequency models were resulted by combining the ultra-low frequency models with the low frequency models from well log data.

2.4 Seismic Pre-Stack Simultaneous Inversion

The seismic pre-stack simultaneous inversion technique that used in this study was based on the constrained sparse spike inversion (CSSI) algorithm. Based on this methodology, a set of elastic property volumes were inverted from multiple seismic angle stacks being input, as shown in Figure 2-9.

ลิขสิทธิ์มหาวิทยาลัยเชียงใหม่
Copyright© by Chiang Mai University
All rights reserved

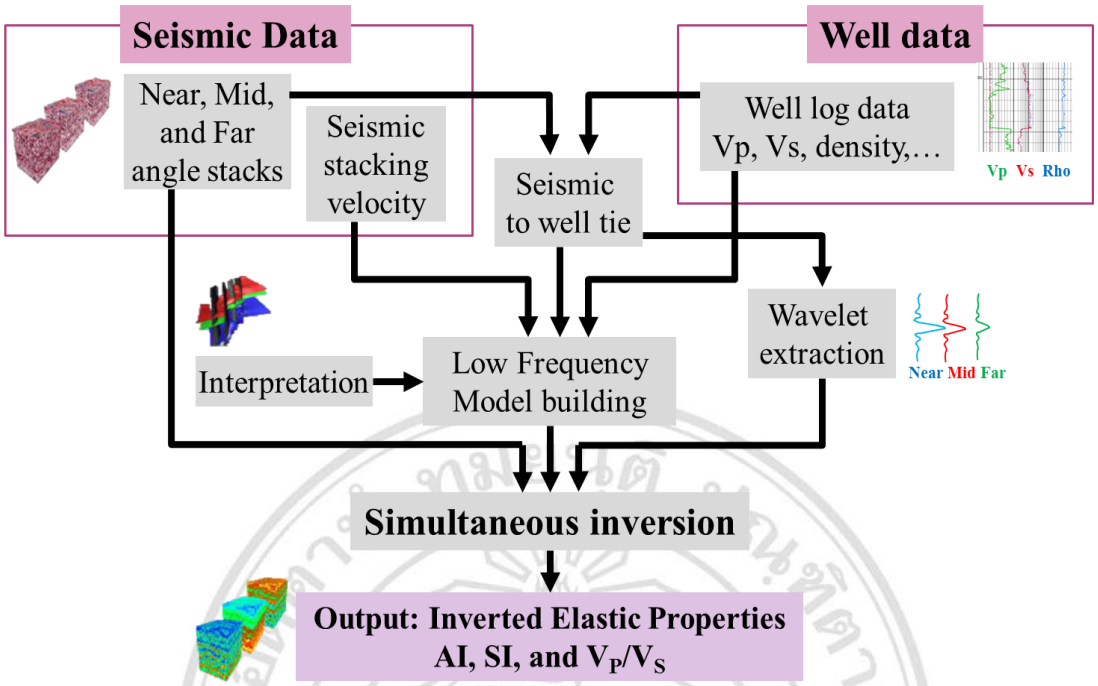

Figure 2-9 Schematic workflow of pre-stack simultaneous inversion.

At each common mid-point location, the seismic data were modelled as the convolution of a set of reflection coefficients, using the extracted wavelets. The reflection coefficients were derived from the elastic properties using Aki-Richards approximation (Aki and Richards, 1980) as Equation 2-11:

$$\mathrm{Rpp}(\theta) = \frac{1}{2}\left(\frac{\Delta \mathrm{Vp}}{\mathrm{Vp}} + \frac{\Delta \rho}{\rho}\right) - 2\frac{\mathrm{Vs}^2}{\mathrm{Vp}^2}\sin^2\theta\left(2\frac{\Delta \mathrm{Vs}}{\mathrm{Vs}} + \frac{\Delta \rho}{\rho}\right) + \frac{1}{2}\tan^2\theta\frac{\Delta \mathrm{Vp}}{\mathrm{Vp}} \qquad (2\text{-}11),$$

where Vp , Vs velocities and ρ density, are averaged across an interface and angle θ is the average of incident and transmitted compressional wave. $\frac{\Delta \mathrm{Vp}}{\mathrm{Vp}}$, $\frac{\Delta \mathrm{Vs}}{\mathrm{Vs}}$ and $\frac{\Delta \rho}{\rho}$ are fractional changes in Vp, Vs and ρ across an interface.

The inversion process was controlled by a set of constraints based on a priori information from the known geology or from well logs. Lateral variations in the low frequencies were incorporated through the use of elastic parameter volumes as trends. The optimal elastic parameters were estimated by minimizing an objective function, leading to the final seismic inversion results, such as acoustic impedance; shear impedance and density cubes. The inverted elastic parameter results were compared to upscaled logs at each well, to evaluate the quality of the results. Residual seismic of all

ลิขสิทธิ์มหาวิทยาลัยเชียงใหม่
Copyright© by Chiang Mai University
All rights reserved

partial stacks were calculated using seismic data subtracted with the modelled synthetic from inverted properties, to consider the seismic misfit for all angle stacks.

2.5 Lithofacies Classification

The probabilistic facies classification using probability density functions (PDFs) was based on Bayes' theorem, combined with analysed rock physics results derived from well log data, as shown in Figure 2-10. Crossplots of AI and Vp/Vs colored with facies types were used to define PDFs in two dimensions. PDFs were applied to the inverted elastic property volumes, to make probability and lithofacies cubes. Conditional probability was computed including all uncertainties in statistical models. More available prior data reduced ambiguity.

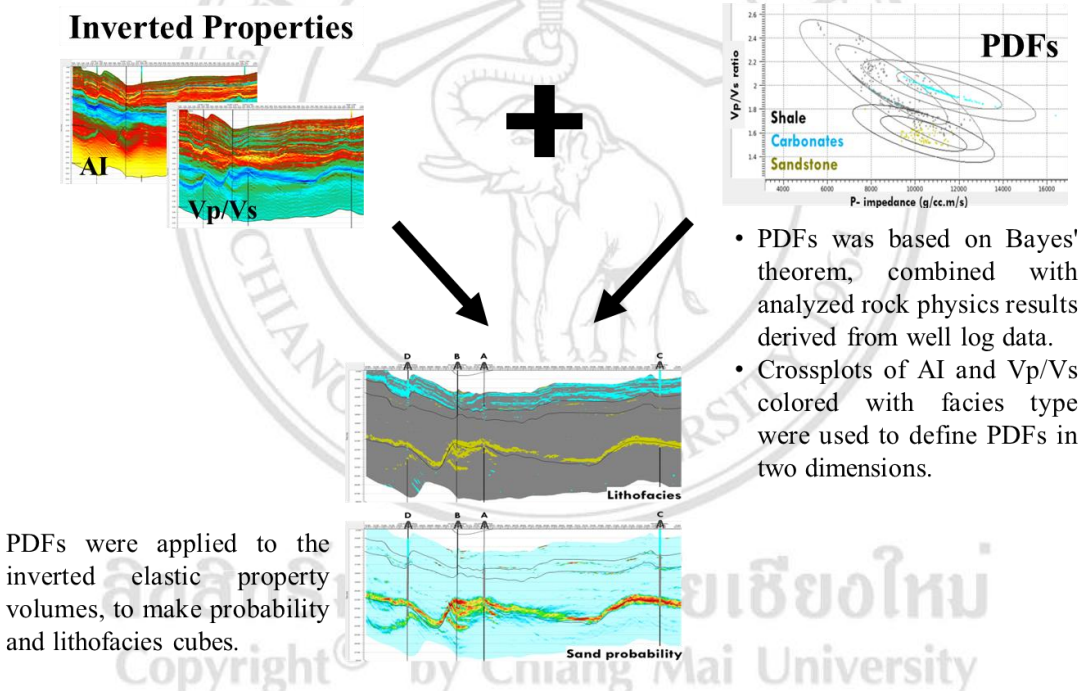

Figure 2-10 Workflow used for lithofacies classification using Bayes' theorem.

ลิขสิทธิ์มหาวิทยาลัยเชียงใหม่
Copyright© by Chiang Mai University
All rights reserved